Chromosome breakage after G2 checkpoint release

Dorothee Deckbar,[1] Julie Birraux,[2] Andrea Krempler,[1] Leopoldine Tchouandong,[1] Andrea Beucher,[1] Sarah Walker,[2] Tom Stiff,[2] Penny Jeggo,[2] and Markus Löbrich[1]

[1]Fachrichtung Biophysik, Universität des Saarlandes, 66421 Homburg/Saar, Germany
[2]Genome Damage and Stability Centre, University of Sussex, East Sussex BN1 9RQ, England, UK

DNA double-strand break (DSB) repair and checkpoint control represent distinct mechanisms to reduce chromosomal instability. Ataxia telangiectasia (A-T) cells have checkpoint arrest and DSB repair defects. We examine the efficiency and interplay of ATM's G2 checkpoint and repair functions. Artemis cells manifest a repair defect identical and epistatic to A-T but show proficient checkpoint responses. Only a few G2 cells enter mitosis within 4 h after irradiation with 1 Gy but manifest multiple chromosome breaks. Most checkpoint-proficient cells arrest at the G2/M checkpoint, with the length of arrest being dependent on the repair capacity. Strikingly, cells released from checkpoint arrest display one to two chromosome breaks. This represents a major contribution to chromosome breakage. The presence of chromosome breaks in cells released from checkpoint arrest suggests that release occurs before the completion of DSB repair. Strikingly, we show that checkpoint release occurs at a point when approximately three to four premature chromosome condensation breaks and ~20 γH2AX foci remain.

Introduction

DNA damage response mechanisms function to maintain genomic stability in normal cells. Because genomic instability is a characteristic of cancer cells, it is evident that at least some of these damage response pathways become impaired during progression to carcinogenesis. Additionally, patients with defective damage response pathways frequently show cancer predisposition, of which ataxia telangiectasia (A-T) is a well-known example. Significant insight has been gained into the roles of individual damage response pathways. Understanding the efficiency as well as the interplay between them is an important next step (Difilippantonio et al., 2000; Gao et al., 2000).

DNA double-strand break (DSB) repair and cell cycle checkpoint arrest represent two pathways to maintain genomic stability (van Gent et al., 2001; Wahl and Carr, 2001; Lieber et al., 2003; Kruhlak et al., 2006; Bekker-Jensen et al., 2006; Mari et al., 2006). A-T mutated (ATM) plays a critical role in regulating cell cycle checkpoint arrest in response to DSBs (Shiloh, 2003; Ward and Chen, 2004; Lou et al., 2006) and regulates a component of DSB repair (Kühne et al., 2004; Riballo et al., 2004). The prevailing evidence suggests that in G0/G1, ATM is required for Artemis, a nuclease, to process a subset (~15%) of radiation-induced DSBs before rejoining. A-T, a disorder caused by mutations in ATM, is associated with pronounced chromosomal instability, cancer susceptibility, and clinical radiosensitivity. This has generally been attributed to ATM's role in cell cycle checkpoint regulation. However, older cytogenetic data (Cornforth and Bedford, 1985; Jeggo et al., 1998) and the recent repair defect described in A-T cells (Riballo et al., 2004) raises the issue of how ATM's repair and checkpoint functions interplay to maintain chromosome stability. Here, we exploit A-T as a model to define the efficiency and dissect the interplay between DNA repair and cell cycle checkpoint pathways, focusing our attention on two ATM-dependent functions, DSB repair in G2 and G2/M checkpoint arrest.

Correspondence to Penny Jeggo: p.a.jeggo@sussex.ac.uk; or Markus Löbrich: markus.loebrich@uniklinik-saarland.de

Abbreviations used in this paper: A-T, ataxia telangiectasia; ATM, A-T mutated; CENP-F, centromere protein F; DSB, double-strand break; FAR, fraction of radioactivity released; IR, ionizing radiation; MEF, mouse embryonic fibroblast; MI, mitotic index; PCC, premature chromosome condensation; PFGE, pulsed-field gel electrophoresis; WT, wild-type.

The online version of this article contains supplemental material.

Results and discussion

ATM- and Artemis-dependent DSB repair operates in G1 and G2

To investigate the contribution of ATM and Artemis to DSB repair in cell cycle phases other than G0, we analyzed asynchronously growing cell cultures to avoid the potential introduction of DSBs during synchronization. In one approach, we used pan-nuclear centromere protein F (CENP-F) staining to identify G2 cells (Liao et al., 1995; Kao et al., 2001; Fig. S1 A, available at http://www.jcb.org/cgi/content/full/jcb.200612047/DC1) and added aphidicolin to prevent S phase cells from progressing into G2 during analysis. Mitotic cells exhibiting distinct centromeric

The Journal of Cell Biology, Vol. 176, No. 6, March 12, 2007 749–755
http://www.jcb.org/cgi/doi/10.1083/jcb.200612047

CENP-F staining and condensed chromatin were excluded from analysis. Under these conditions, S phase cells do not progress into G2 (Fig. S1 B) and a considerable proportion of cells irradiated with 1.5 Gy x-rays remain positive for pan-nuclear CENP-F staining for 6–8 h (i.e., they remain in G2), providing sufficient time to detect the ATM/Artemis repair defect, which is measurable at >4 h after irradiation in G0 cells.

Enumeration of γH2AX foci in aphidicolin-treated CENP-F–positive primary human fibroblasts after 1.5 Gy x-irradiation demonstrated that ATM- and Artemis-dependent DSB repair operates in G2 (Fig. 1 A). Aphidicolin treatment did not affect the repair capacity of G2 cells (Fig. S1 C) but caused pronounced H2AX phosphorylation in cells that were CENP-F negative but positive for the S/G2 marker, cyclin A, most likely because of the activation of ATR after replication arrest (Fig. S1 A). Enumeration of γH2AX foci in CENP-F–negative cells that were also negative for the pronounced, aphidicolin-induced γH2AX phosphorylation allowed the analysis of repair in G1 phase cells (Fig. 1 A). For all cell lines, we observed similar kinetics and magnitude of repair in G1 and G2, which was also similar to that previously observed in G0 cells (Riballo et al., 2004). Foci numbers correlated with DNA content being twice as high in G2 compared with G1 (Fig. 1 A). In analogy to our previous study (Riballo et al., 2004), we confirmed that ATM and Artemis operate in the same repair pathway by analyzing the repair defect in Artemis cells treated with the specific ATM small molecule inhibitor KU55933 (Hickson et al., 2004). The dual deficiency in Artemis and ATM did not cause an increased repair defect relative to the defect in Artemis cells (Fig. 1 B). Thus, ATM and Artemis are epistatic in G1 and G2 and function to repair a subfraction of DSBs similar to that observed in confluent cells. Because our results were obtained with nonisogenic human cell lines, we also investigated γH2AX foci formation in matching wild-type (WT), A-T, and Artemis mouse embryonic fibroblasts (MEFs) using procedures similar to those used with human cells and observed identical repair kinetics (Fig. S1 D).

To substantiate that γH2AX foci analysis monitors DSB repair, we developed and applied a pulsed-field gel electrophoresis (PFGE) technique to monitor DSB repair specifically in G2 phase cells (Fig. 1 C). Exponentially growing primary human fibroblasts were pulse-labeled with [methyl-^{3}H]thymidine for 1 h and irradiated with 80 Gy 4 h after labeling (when in G2; Fig. S1 E). After 48 and 72 h of repair, cells were harvested and the fraction of radioactivity released (FAR) from the gel plug

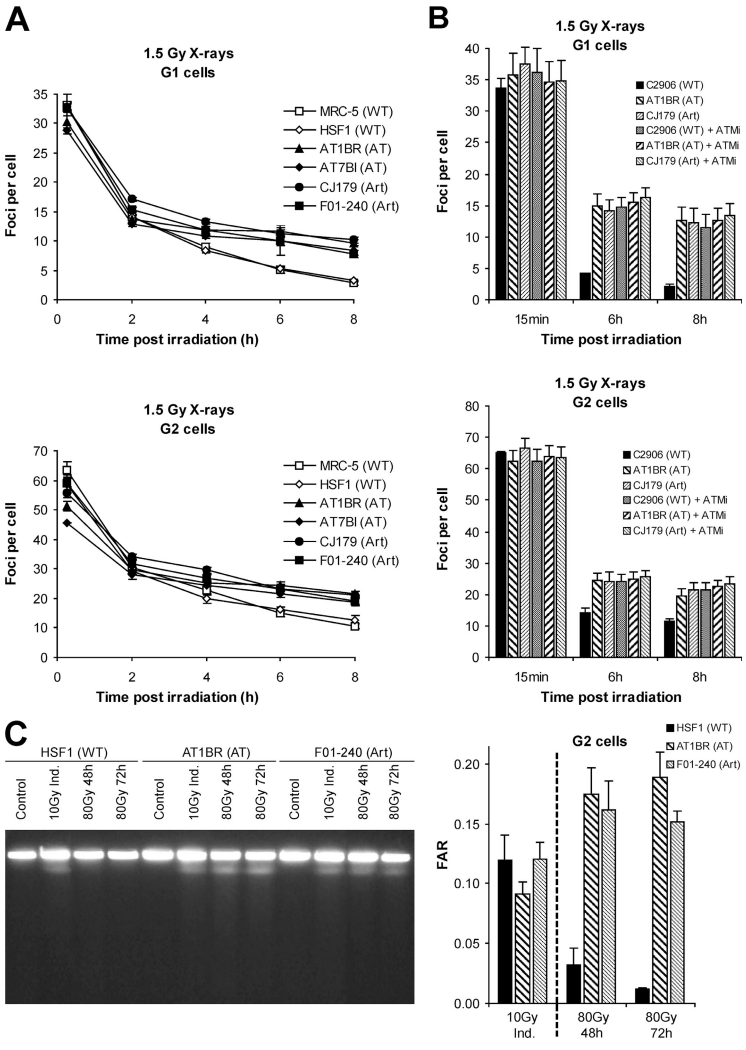

Figure 1. **A-T and Artemis primary human fibroblasts exhibit a DSB repair defect in G1 and G2.** (A) γH2AX foci analysis in G1 and G2 phase cells after 1.5 Gy x-irradiation. Background foci numbers were ∼2 in G2 and 0.2 in G1. (B) γH2AX foci analysis in G1 and G2 phase cells after 1.5 Gy x-irradiation in the absence or presence of the ATM small molecule inhibitor KU55933 (ATMi). (C) FAR assay of [methyl-^{3}H]thymidine-labeled exponentially growing cells irradiated in G2. (left) Ethidium bromide–stained PFGE gel from primary human fibroblasts irradiated with 10 Gy (for assessing DSB induction) or 80 Gy (for 48- and 72-h repair points) x-rays. The image has been grouped from different parts of the same gel for clarity. Note that the ethidium bromide signal represents DNA from all cells (G1, S, and G2) and is not used for evaluation. (right) FAR values calculated from the scintillation counts of gel slices derived from PFGE gels. Error bars indicate SEM.

into the gel was quantified by liquid scintillation counting. The FAR values after repair incubation provide an estimate of the level of unrepaired DSBs and can be compared with FAR values obtained from samples analyzed immediately after irradiation without repair. FACS analysis of parallel samples labeled with BrdU instead of [methyl-^{3}H]thymidine showed that labeled cells have progressed to late S/G2 at the time of irradiation (4 h after labeling) and remained in G2 for at least 72 h after irradiation with 80 Gy (Fig. S1 E). We obtained a similar level of unrepaired DSBs in A-T and Artemis cells, which was similar to (or slightly higher than) the level of DSBs induced in cells irradiated with 10 Gy and not incubated for repair (i.e., ~1/8 of the DSBs induced by 80 Gy remain unrepaired; Fig. 1 C). Thus, the magnitude of the G2 repair defect measured by PFGE is similar to the ~15% repair defect observed by γH2AX foci analysis of G2 or G1 cells (Fig. 1 A) and confluent cells (Riballo et al., 2004). The identical repair defect of A-T and Artemis cells in G2 and G1 is perhaps surprising, given that ATM has been reported to be required for homologous recombination. One possible explanation is that Artemis has a role in DSB repair processes other than nonhomologous end joining. Alternatively, our findings could indicate that the majority of ionizing radiation (IR)–induced DSBs are repaired by nonhomologous end joining in G1 and G2. In support of this, we have observed that DNA ligase IV– and Ku80-deficient MEFs have a similar, major DSB repair defect in G1 and G2 (unpublished data).

Artemis cells show normal checkpoint induction and prolonged G2/M arrest

Previously, we presented evidence that Artemis cells show normal G2/M checkpoint activation assessed by counting mitotic cells up to 9 h after IR (Riballo et al., 2004). Subsequently, Zhang et al. (2004), using phosphoH3 FACS analysis, concluded that cells treated with Artemis siRNA show premature release from the G2/M checkpoint, implicating Artemis in IR-induced checkpoint responses. To examine the maintenance as well as the activation of G2/M arrest, we counted mitotic cells up to 24 h after IR in cells treated with nocodazole to accumulate cells in mitosis. We confirm that Artemis cells, in contrast to A-T cells, show normal G2/M checkpoint induction and, importantly, remain arrested for the same length and possibly greater than WT cells (Fig. S2 A, available at http://www.jcb.org/cgi/content/full/jcb.200612047/DC1).

We next analyzed the G2/M checkpoint by phosphoH3 FACS analysis and observed checkpoint activation in Artemis but not A-T cells (Fig. 2 A). WT cells were released from checkpoint arrest 4–6 h after 1.3 Gy and 12 h after 6 Gy x-irradiation. Artemis cells were released slightly later after 1.3 Gy and failed to be released for at least 16 h after 6 Gy (Fig. 2 A and Fig. S2 B). Normal checkpoint induction and a prolonged arrest at the G2/M border was also observed in irradiated Artemis MEFs compared with WT MEFs (Fig. 2 B). We also evaluated the time course for the progression of G2 cells through mitosis into G1 by analyzing BrdU-labeled cells. Exponentially growing fibroblasts were pulse-labeled with BrdU for 1 h and irradiated with 1 Gy 4 h after labeling (when in G2). G2/M checkpoint arrest results in the retention of BrdU-labeled cells in G2. Quantification of the BrdU-labeled G2 cells for up to 12 h after irradiation confirmed that Artemis cells exhibit a prolonged G2/M arrest (Fig. 2 C). The prolonged arrest of Artemis cells in Fig. 2 was less evident in the experiments involving mitotic counting (Fig. S2 A), which may reflect the use of nocodazole in the latter approach, which delays reentry from G2/M arrest. Our observation of a prolonged arrest in Artemis cells is consistent with a role of Artemis in DSB repair in G1 and G2. One explanation for the difference between our results and those of Zhang et al. (2004) is that their study used human tumor cells for siRNA knock down of Artemis. Such cells frequently behave aberrantly because of abnormal levels of Chk1/Chk2 or cell cycle checkpoint regulation.

ATM's G2 checkpoint and repair functions both contribute to the avoidance of chromosome breakage

Having established that Artemis affects ATM's role in G2 DSB repair but not its function in G2 checkpoint control, we wished to evaluate the contribution of these two ATM functions to the prevention of chromosome aberrations in primary human WT, A-T, and Artemis fibroblasts (Fig. 3). We focused on chromosome breaks arising from G2-irradiated cells by adding aphidicolin to prevent S phase cells from progressing into G2 during analysis. Growing cell populations were irradiated with 1 Gy

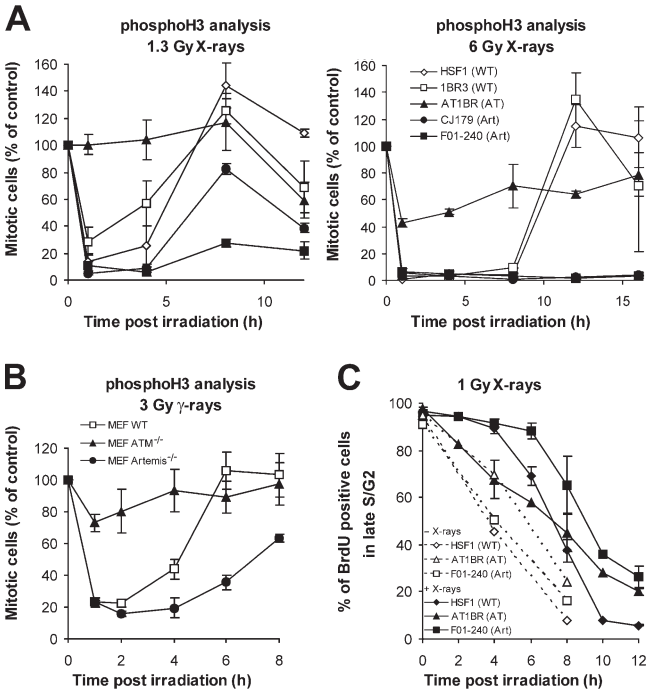

Figure 2. **Artemis cells show proficient checkpoint induction and a prolonged G2/M arrest.** (A) PhosphoH3 analysis of primary human fibroblasts after 1.3 and 6 Gy x-irradiation. (B) PhosphoH3 analysis of MEFs after 3 Gy γ-irradiation. Data shown are the percentage of mitotic cells relative to unirradiated cells at time 0. (C) FACS analysis of BrdU-labeled primary human fibroblasts. The percentage of BrdU-positive cells in late S/G2 was assessed up to 12 h after 1 Gy x-irradiation given at 4 h after BrdU labeling (i.e., when BrdU-labeled cells have progressed into late S/G2). Dotted lines represent the percentage of BrdU-positive cells in late S/G2 without irradiation. Error bars indicate SEM.

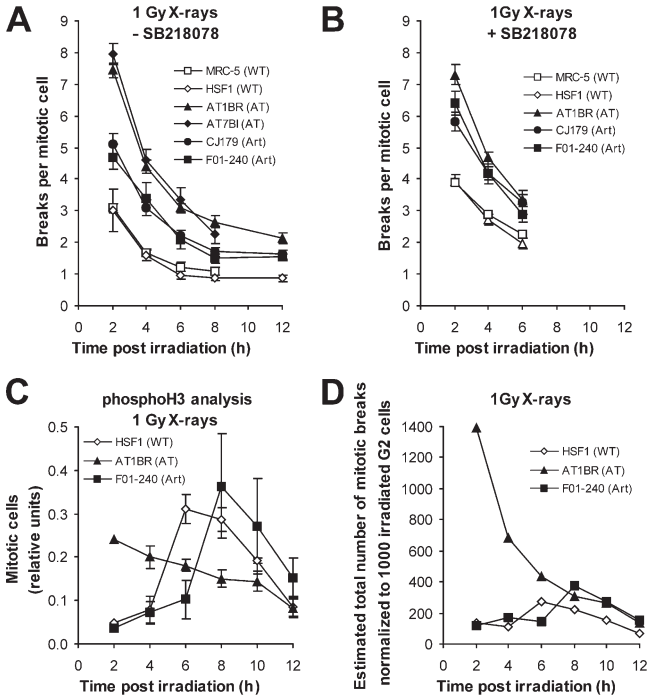

Figure 3. **ATM's repair and checkpoint functions contribute to prevent chromosome breakage.** (A) Chromosome breaks per mitotic cell in metaphase spreads from primary human fibroblasts harvested at varying times after 1 Gy x-irradiation in the presence of aphidicolin. Breaks in unirradiated samples were <0.1 and were subtracted from the breaks in the irradiated samples. (B) Same analysis as in A in the presence of the Chk1/2 inhibitor SB218078. SB218078 did not cause chromosome breaks in unirradiated cells. (C) PhosphoH3 analysis of primary human fibroblasts after 1 Gy x-irradiation in the presence of aphidicolin (i.e., the same conditions used for the chromosomal analysis). The measured MIs were normalized to provide the same integral value of 1 for all three cell lines. (D) Estimation of the kinetics for total mitotic chromosome breakage. The values are derived from the number of chromosome breaks per mitotic cell for cells that enter mitosis at specific time points (taken from A) multiplied by the number of cells reaching mitosis at these times (taken from C). Error bars indicate SEM.

and analyzed for chromosome breaks per mitotic cell at early times (2 and 4 h) after IR, similar to that undertaken in previous studies (Kemp and Jeggo, 1986). In all cell lines, chromosome breaks decreased with time reflecting DSB repair (Fig. 3, A and B). A-T cells show a pronounced elevation of the number of chromosome breaks per mitotic cell (approximately threefold higher than WT cells), whereas Artemis cells exhibit about twofold more breaks per cell than WT cells, consistent with Artemis's repair function in G2 (Fig. 3 A). Thus, a combined checkpoint and repair defect is more severe than a repair defect alone.

We also evaluated the contribution of repair and checkpoint loss to chromosome aberration formation by using the checkpoint inhibitor SB218078. This drug has been described to impact upon Chk1 activity (Zhao et al., 2002) and abolishes 53BP1 foci formation after hydroxyurea treatment, a Chk1-dependent phenotype (Fig. S3 A, available at http://www.jcb.org/cgi/content/full/jcb.200612047/DC1; Sengupta et al., 2004). Addition of SB218078 completely abolished the G2/M checkpoint response in primary human fibroblasts as well as in MEFs (Fig. S3, B and C), whereas repair of IR-induced DSBs in G2 remained unaffected (Fig. S3 D). SB218078 had no effect on chromosome aberration formation in A-T cells but increased the level of chromosome breaks per cell in Artemis cells to that of A-T cells (Fig. 3 B). WT cells treated with SB218078 showed considerably fewer breaks per cell than drug-treated A-T or Artemis cells, which represents the contribution of ATM/Artemis-dependent DSB repair to the prevention of chromosome aberrations in the absence of checkpoints. It is noteworthy that the cells forming chromosome aberrations are those in G2 at the time of irradiation, as the addition of aphidicolin prevented S phase cells from progressing into G2 during analysis. Thus, any role of Chk1 in replication fork stability will not affect chromosome aberration formation. Moreover, SB218078 did not cause chromosome breaks in the absence of IR.

Cells released from the G2/M checkpoint exhibit chromosome aberrations in mitosis

Our studies predict that 1 Gy–irradiated G2 phase Artemis cells would harbor 9–12 DSBs that remain unrepaired for prolonged times. The release of Artemis cells from G2/M checkpoint arrest 6–8 h after irradiation suggested that the G2/M checkpoint might be unable to detect 9–12 DSBs. To investigate whether DSB repair is complete at the point of checkpoint release, we evaluated chromosome aberrations in mitotic cells that arise after checkpoint release (i.e., at time points >4 h after IR; Fig. 3). Because WT and Artemis cells progress from G2 into G1 within 12 h after IR with 1 Gy (see Fig. 2 C), we evaluated chromosome breakage up to this time point. Strikingly, the level of chromosome aberrations in WT and Artemis cells at times when the cells that had initiated the checkpoint leave G2 (4–8 h in WT and 6–10 h in Artemis) is approximately one to two breaks per cell (Fig. 3 A), which is >10-fold above the background number of chromosome breaks. Thus, almost all cells released from the G2 checkpoint exhibit chromosome aberrations in mitosis. This observation represents direct experimental evidence that the human G2/M checkpoint is not maintained until the completion of repair.

This prompted us to investigate the time course for the appearance of chromosome aberrations in mitosis. Cells entering mitosis at early times exhibit more chromosome breaks than cells entering at later times (Fig. 3 A). However, this analysis fails to consider the number of cells reaching mitosis at each time point. Thus, we assessed the number of cells reaching mitosis under the same conditions used for our chromosomal studies (i.e., in the presence of aphidicolin) by using phosphoH3 FACS analysis (Fig. 3 C) and estimated the total number of mitotic chromosome breaks by multiplying the chromosome breaks per cell by the number of mitotic cells (Fig. 3 D; see Materials and methods for details of this estimation). Considering this novel concept, we examined the kinetics for mitotic chromosome breakage and observed a maximum at times after the G2/M checkpoint has been released (i.e., at 6–8 h in WT and at 8–10 h in Artemis cells). Thus, cells released from the checkpoint (at ≥6 h after IR) as opposed to cells that escape checkpoint arrest at early times (at ≤4 h after IR) represent a major cause of mitotic chromosome breakage (Fig. 3 D). We also evaluated the number of cells reaching mitosis from the progression

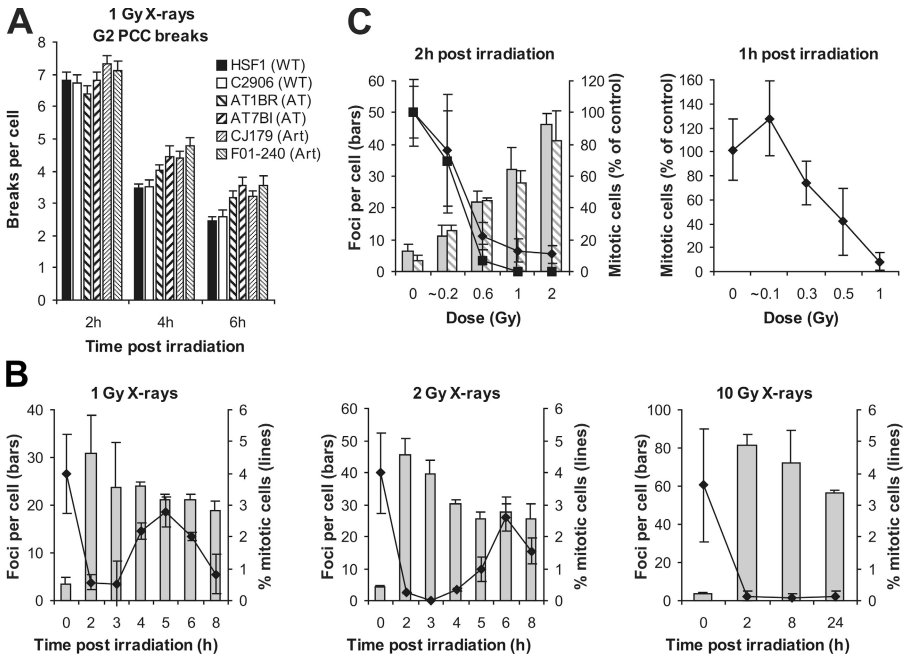

Figure 4. **The G2/M checkpoint has a threshold of ∼3.5 PCC breaks and ∼20 γH2AX foci.** (A) Analysis of G2 PCC chromosomal breaks in calyculin A–treated cells in the presence of aphidicolin at 2, 4, and 6 h after 1 Gy x-irradiation. Breaks in unirradiated samples were <0.2 and were subtracted from the breaks in the irradiated samples. $P < 0.01$ (*t* test) for AT1BR, AT7BI, CJ179, and F01-204 compared with HSF1 or C2906 at 4 and 6 h (but not at 2 h). (B) γH2AX analysis and mitotic counting of transformed MRC-5V1 fibroblasts at varying times after 1, 2, and 10 Gy x-irradiation in the presence of aphidicolin. The analysis was done on the same samples by counting the fraction of phosphoH3-positive mitotic cells and foci numbers in CENP-F–positive G2 cells, respectively. The pronounced decline in MI at 8 h after 1 and 2 Gy likely reflects the depletion of G2 cells. (C, left) Same analysis as in B evaluating transformed (MRC-5V1; gray bars, diamonds) and immortalized (48BR hTert; shaded bars, squares) fibroblasts 2 h after 0, 0.2, 0.6, 1, and 2 Gy x-irradiation. (right) PhosphoH3 analysis of primary (48BR) fibroblasts after 0, 0.1, 0.3, 0.5, and 1 Gy x-irradiation by FACS. γH2AX foci were scored on parallel samples and provided similar numbers to those of MRC-5V1 and 48BR hTert cells. Analysis was performed 1 h after IR, as pilot experiments showed that primary cells show a more rapid onset of checkpoint arrest. Note that very short exposure times were required to deliver the low doses in these experiments, resulting in potential errors in the estimated dosimetry. Error bars indicate SEM.

of BrdU-labeled G2 cells (obtained from Fig. 2 C). An estimation of the kinetics for mitotic chromosome breakage using this analysis provided similar results to that using the phosphoH3 FACS data (Fig. S3 E). Thus, the concept of evaluating chromosome breakage by considering breaks per mitotic cell as well as the number of mitotic cells reveals the striking finding that checkpoint release before the completion of repair represents a major cause for chromosome aberration formation. Remarkably, the total number of breaks in released cells is similar in WT and Artemis cells, although they arise with delayed kinetics in the repair-defective cells. The decrease in breaks at prolonged times after treatment (>10 h) is due to the depletion of irradiated G2 cells; i.e., nearly all cells have left G2. A-T cells display entirely different kinetics. Because of the lack of checkpoint arrest, they display an elevated number of chromosome breaks that decreases with time in part because of DSB repair and the rapid depletion of the G2 population.

The G2/M checkpoint has a defined threshold

Our findings establish that all cells released from the G2 checkpoint harbor unrepaired damage, strongly suggesting that the G2/M checkpoint has a threshold. Our observation that Artemis cells remain checkpoint arrested longer than WT cells (Fig. 2) but are released with a similar number of γH2AX foci (Fig. 1 A) or mitotic chromosome breaks (Fig. 3 A) supports this notion. However, we sought other procedures to confirm the presence of DSBs in G2 at the time of checkpoint release and to evaluate the sensitivity limit of the G2 checkpoint. As one approach, we performed premature chromosome condensation (PCC) of G2 cells using the phosphatase inhibitor calyculin A (Fig. 4 A). G2 cells are readily distinguished from mitotic cells and allow the analysis of PCC breaks (Asakawa and Gotoh, 1997). At 4 and 6 h after 1 Gy x-irradiation, the time at which checkpoint release commences in WT and Artemis cells, respectively, we observed three to four PCC breaks per cell consolidating the presence of DSBs at the time of checkpoint release (Fig. 4 A). Moreover, WT cells at 4 h and Artemis cells at 6 h harbor a similar number of PCC breaks. Interestingly, these studies also provide an additional demonstration of a repair defect in Artemis cells. Previous studies equating PCC breaks with DSBs estimated by PFGE have reported a 1:3–6 relationship (i.e., 3–6 DSBs equate to 1 PCC break; Cornforth and Bedford, 1993). Thus, our PCC data suggest a sensitivity level of 10–20 DSBs.

We also used γH2AX foci as a further marker to determine whether DSB repair is complete at the time of checkpoint release. We scored the number of foci in CENP-F–positive G2 phase cells at differing times after IR and, in the same population of cells, counted the number of mitotic cells (Fig. 4 B). We used exponentially growing transformed human fibroblasts, which provide a high mitotic index (MI). Mitotic cells were scored as phosphoH3-positive cells with condensed chromatin. Consistent with these findings, we observed that checkpoint duration increases with dose and that cells are released from the checkpoint with ∼20 foci (Fig. 4 B). Similar results were obtained with hTert-immortalized fibroblasts (unpublished data). We also analyzed mitotic cells at the 6-h time point and observed foci numbers similar to those of G2 cells, demonstrating that the cells released from the checkpoint do enter mitosis with foci and that there is no selection for cells exiting the checkpoint (Fig. S3 F; Rothkamm et al., 2003; Syljuasen et al., 2006). Previously, we and others have observed a 1:1 relationship between γH2AX foci and DSBs (Rogakou et al., 1999; Redon et al., 2002; Rothkamm and Löbrich, 2003). Although it is possible that γH2AX foci analysis could overestimate DSBs remaining if

repair is completed before the loss of visible foci, this is unlikely to occur in Artemis-deficient cells, where unrepaired DSBs persist for many days in G1 and G2. Thus, our studies analyzing γH2AX foci are consistent with a threshold of 10–20 DSBs. Additionally, our PFGE studies with G2 (Fig. 1 C), and previously with G0 cells, show that ∼15% of the induced DSBs remain unrepaired in Artemis cells for many days. PFGE studies estimated 30–40 DSBs induced per Gy in G1 (Cedervall et al., 1995; Löbrich et al., 1995). Because G2 Artemis cells irradiated with 1 Gy are completely released from G2 by 12 h, the estimated persisting damage level (15% of 60–80 DSBs induced: 9–12 DSBs) is unable to maintain the checkpoint. In contrast, after 6 Gy, the level of DSBs remaining exceeds the threshold and results in arrest being maintained for at least 16 h. Hence, our PFGE data, which do not rely on γH2AX foci analysis, also indicate that the G2/M checkpoint threshold is >9–12 DSBs.

To evaluate whether induction of the G2/M checkpoint has a similar sensitivity limit, we analyzed transformed and immortalized fibroblasts exposed to doses up to 2 Gy at 2 h after irradiation, the earliest time point at which we observed complete arrest in pilot experiments (Fig. 4 C). Cells irradiated with 0.6 Gy or higher show complete checkpoint arrest. The foci level 2 h after 0.6 Gy is ∼20. Lower levels cause a partial arrest (Fig. 4 C). Because repair occurs during the 2-h incubation necessary to measure checkpoint induction, our findings are consistent with a level of ∼20 foci being required to activate checkpoint arrest. We also considered it important to examine primary human cells. The low MI of primary cells necessitated FACS analysis to estimate MI, precluding a parallel evaluation of γH2AX foci formation. Our findings were similar to those obtained using transformed/immortalized cells (Fig. 4 C). Importantly, use of a lower dose, inducing <10 γH2AX foci did not induce any detectable arrest. Based on 30–40 DSBs induced per Gy in G1, 20 DSBs are induced after doses of 0.25–0.33 Gy in G2 cells. This correlates with the mild checkpoint induction observed here after 0.2–0.3 Gy and the absence of checkpoint arrest after 0.1 Gy (Fig. 4 C). Thus, these findings are consistent with a similar threshold number of DSBs (10–20) both activating and maintaining checkpoint arrest. The existence of a threshold for G2/M checkpoint arrest provides a potential explanation for low-dose hypersensitivity, a phenomenon describing exquisite cellular sensitivity at low radiation doses (Marples et al., 2004). Indeed, a G2/M threshold of ∼20 DSBs would predict the reported survival responses.

In conclusion, we have examined the efficacy of ATM's repair and checkpoint functions in G2 and dissected the contribution of these two ATM functions to the avoidance of chromosomal breakage. We demonstrate that (1) the kinetics of DSB repair in G2 is similar to that in G1 and that A-T and Artemis cells display an epistatic repair defect in G2 identical to that in G1; (2) Artemis cells are G2/M checkpoint proficient; (3) chromosome breaks occur 0–4 h after IR in a small fraction of cells that fail to arrest at the G2/M checkpoint; (4) the majority of cells arrest at the G2/M checkpoint but give rise to one to two chromosome breaks upon release. This represents a major cause of chromosome aberration formation; and (5) the G2/M checkpoint has a defined threshold, which we estimate to be approximately three to four PCC breaks or ∼10–20 DSBs. This threshold allows for the generation of one to two chromosome breaks in mitosis.

Materials and methods

Cell culture, chemicals, and irradiation

Cells were grown as described previously (Riballo et al., 2004). 10, 15, or 20% FCS was used depending on the cell line. For the FAR assay, cells were labeled with 37 kBq/ml [methyl-^{3}H]thymidine (2.81 TBq/mmol; GE Healthcare) for 1 h (electrophoresis was performed according to Kühne et al. [2004]). Aphidicolin and nocodazole (Sigma-Aldrich) were added at 3 μg/ml and 100 ng/ml, respectively. Inhibition of Chk1 activity was achieved by addition of 2.5 μM SB218078 (Calbiochem) 30 min before IR. ATMi (KU55933; provided by G. Smith, KuDos Pharmaceuticals Ltd, Cambridge, UK) was added at 10 μM 30 min before IR. X-irradiation was performed at 90 or 120 kV, γ-irradiation using a ^{137}Cs-source. Dosimetry was performed with ion chambers and considered the increase in dose for cells grown on glass coverslips relative to plastic surfaces.

Metaphase spreads and PCC

To collect metaphases, 100 ng/ml colcemid (Sigma-Aldrich) was added 2 h before harvesting (1 h for the 2-h time point and 4 h for the 12-h time point). For PCC analysis, cells were treated with 50 ng/ml calyculin A (Calbiochem) for 30 min before harvesting. Chromatid breaks and excess fragments (counted as two chromatid breaks) were scored in 20–100 chromosome spreads from at least three independent experiments per data point.

FACS

Cells pulse-labeled with 10 μM BrdU (Roche) for 1 h were analyzed according to standard protocols. For phosphoH3 staining, cells were permeabilized with PBS/0.25% Triton X-100 (15 min on ice), incubated in 100 μl α-phosphoH3 antibody (Ser10; 7.5 μg/ml PBS/1% BSA; Upstate Biotechnology) overnight, and treated with the Alexa Fluor 488–conjugated goat α-mouse (MoBiTec) or an FITC-conjugated swine α-rabbit antibody (DakoCytomation) in PBS/1% BSA for 1 h, followed by 50 μg/ml propidium iodide containing 0.5 mg/ml RNase in PBS for 30 min at room temperature. Analysis was performed on a FACScan or FACSCalibur using the CellQuest software (Becton Dickinson).

Immunofluorescence

Cells grown on coverslips were fixed in 100% methanol (−20°C) for 30 min, permeabilized in acetone (−20°C) for 1 min, and washed three times for 10 min in PBS/1% FCS. Samples were incubated with primary antibodies (monoclonal or polyclonal α-γH2AX antibody [1:200; Upstate Biotechnology], polyclonal α–CENP-F and α–cyclin A antibody [1:200; Santa Cruz Biotechnology, Inc.], or polyclonal α-phosphoH3 antibody [Ser10; 1:200; Upstate Biotechnology]) in PBS/1% FCS for 1 h at room temperature, washed in PBS/1% FCS three times for 10 min, and incubated with Alexa Fluor 488–, Alexa Fluor 546–, or Alexa Fluor 594–conjugated secondary antibodies (1:500; MoBiTec) for 1 h at room temperature. Cells were washed in PBS four times for 10 min and mounted using Vectashield mounting medium containing 4,6 diamidino-2-phenylindole (Vector Laboratories). In a single experiment, cell counting was performed until at least 40 cells and 40 foci were registered per sample. Each data point represents two to three independent experiments. Error bars represent the SEM between the different experiments.

Estimation of the kinetics for total chromosome breakage

Fig. 3 D aims to compare the time course for total mitotic chromosome breakage for three different cell lines: A-T, Artemis, and WT. We have measured for all three lines the MI at defined times after irradiation by phosphoH3 FACS analysis under the same conditions used for the chromosomal analysis, i.e., in the presence of aphidicolin (Fig. 3 C). However, different cell lines can vary considerably in their fraction of G2 phase cells. Moreover, the majority but not all G2-irradiated cells leave G2 within 12 h with slight differences between the three cell lines (Fig. 2 C). We have considered the first variation (different G2 proportions) by normalizing the phosphoH3 data in Fig. 3 C such that the sum of the MIs measured up to 12 h after irradiation is the same for all three cell lines and the second variation by multiplying these MIs with the measured proportion of G2-irradiated cells that leave G2 within 12 h. The latter values are derived from Fig. 2 C.

For example, Artemis cells entering mitosis at 8 h after IR exhibit ~1.5 breaks per mitotic cell (Fig. 3 A). At this time, the relative MI for Artemis cells is ~0.35. Thus, we multiplied the value of 1.5 by 1,000 (to normalize it to 1,000 irradiated G2 cells), by 0.75 (because 75% of all irradiated G2 Artemis cells leave G2 within 12 h; Fig. 2 C), and finally by 0.35 (because 35% of all cells that leave G2 within 12 h do this at the 8-h time point). This provides a value of ~400 mitotic breaks for Artemis cells at 8 h (Fig. 3 D).

Online supplemental material

Fig. S1 provides additional information for the experimental procedures used to measure DSB repair in G2 and shows that A-T and Artemis MEFs exhibit a DSB repair defect in G1 and G2. Fig. S2 provides additional information that Artemis cells show normal G2/M checkpoint induction and a prolonged arrest by counting mitotic cells and by using phosphoH3 FACS analysis. Fig. S3 shows that the Chk1-inhibiting drug SB218078 abolishes the G2/M checkpoint without affecting IR-induced DSB repair in G2 and provides evidence that cells released from G2/M checkpoint arrest exhibit chromosome breaks and γH2AX foci in mitosis. Online supplemental material is available at http://www.jcb.org/cgi/content/full/jcb.200612047/DC1.

The M. Löbrich laboratory is supported by the Deutsche Forschungsgemeinschaft (grant LO 677/4-1/2 and Graduiertenkolleg 377/3), the Bundesministerium für Bildung und Forschung via the Forschungszentrum Karlsruhe (grants 02S8132 and 02S8335), and the Deutsche Zentrum für Luft und Raumfahrt e.V. (grant 50WB0017). The P. Jeggo laboratory is supported by the Medical Research Council, the Human Frontiers Science Programme, the Primary Immunodeficiency Association, the Leukaemia Research Fund, and the European Union (grant FIGH-CT-200200207).

Submitted: 8 December 2006
Accepted: 11 February 2007

References

Asakawa, Y., and E. Gotoh. 1997. A method for detecting sister chromatid exchanges using prematurely condensed chromosomes and immunogold-silver staining. *Mutagenesis.* 12:175–177.

Bekker-Jensen, S., C. Lukas, R. Kitagawa, F. Melander, M.B. Kastan, J. Bartek, and J. Lukas. 2006. Spatial organization of the mammalian genome surveillance machinery in response to DNA strand breaks. *J. Cell Biol.* 173:195–206.

Cedervall, B., R. Wong, N. Albright, J. Dynlacht, P. Lambin, and W.C. Dewey. 1995. Methods for the quantification of DNA double-strand breaks determined from the distribution of DNA fragment sizes measured by pulsed-field gel electrophoresis. *Radiat. Res.* 143:8–16.

Cornforth, M.N., and J.S. Bedford. 1985. On the nature of a defect in cells from individuals with ataxia-telangiectasia. *Science.* 227:1589–1591.

Cornforth, M.N., and J.S. Bedford. 1993. Ionizing radiation damage and its early development in chromosomes. *In* Advances in Radiation Biology, vol. 17. J.T. Lett and W.K. Sinclair, editors. Academic Press, San Diego. 423–496.

Difilippantonio, M.J., J. Zhu, H.T. Chen, E. Meffre, M.C. Nussenzweig, E.E. Max, T. Ried, and A. Nussenzweig. 2000. DNA repair protein Ku80 suppresses chromosomal aberrations and malignant transformation. *Nature.* 404:510–514.

Gao, Y., D.O. Ferguson, W. Xie, J.P. Manis, J. Sekiguchi, K.M. Frank, J. Chaudhuri, J. Horner, R.A. DePinho, and F.W. Alt. 2000. Interplay of p53 and DNA-repair protein XRCC4 in tumorigenesis, genomic stability and development. *Nature.* 404:897–900.

Hickson, I., Y. Zhao, C.J. Richardson, S.J. Green, N.M. Martin, A.I. Orr, P.M. Reaper, S.P. Jackson, N.J. Curtin, and G.C. Smith. 2004. Identification and characterization of a novel and specific inhibitor of the ataxia-telangiectasia mutated kinase ATM. *Cancer Res.* 64:9152–9159.

Jeggo, P.A., A.M. Carr, and A.R. Lehmann. 1998. Splitting the ATM: distinct repair and checkpoint defects in ataxia-telangiectasia. *Trends Genet.* 14:312–316.

Kao, G.D., W.G. McKenna, and T.J. Yen. 2001. Detection of repair activity during the DNA damage-induced G2 delay in human cancer cells. *Oncogene.* 20:3486–3496.

Kemp, L.M., and P.A. Jeggo. 1986. Radiation-induced chromosome damage in X-ray-sensitive mutants (xrs) of the Chinese hamster ovary cell line. *Mutat. Res.* 166:255–263.

Kruhlak, M.J., A. Celeste, G. Dellaire, O. Fernandez-Capetillo, W.G. Muller, J.G. McNally, D.P. Bazett-Jones, and A. Nussenzweig. 2006. Changes in chromatin structure and mobility in living cells at sites of DNA double-strand breaks. *J. Cell Biol.* 172:823–834.

Kühne, M., E. Riballo, N. Rief, K. Rothkamm, P.A. Jeggo, and M. Löbrich. 2004. A double-strand break repair defect in ATM-deficient cells contributes to radiosensitivity. *Cancer Res.* 64:500–508.

Liao, H., R.J. Winkfein, G. Mack, J.B. Rattner, and T.J. Yen. 1995. CENP-F is a protein of the nuclear matrix that assembles onto kinetochores at late G2 and is rapidly degraded after mitosis. *J. Cell Biol.* 130:507–518.

Lieber, M.R., Y. Ma, U. Pannicke, and K. Schwarz. 2003. Mechanism and regulation of human non-homologous DNA end-joining. *Nat. Rev. Mol. Cell Biol.* 4:712–720.

Löbrich, M., B. Rydberg, and P.K. Cooper. 1995. Repair of x-ray-induced DNA double-strand breaks in specific Not I restriction fragments in human fibroblasts: joining of correct and incorrect ends. *Proc. Natl. Acad. Sci. USA.* 92:12050–12054.

Lou, Z., K. Minter-Dykhouse, S. Franco, M. Gostissa, M.A. Rivera, A. Celeste, J.P. Manis, J. van Deursen, A. Nussenzweig, T.T. Paull, et al. 2006. MDC1 maintains genomic stability by participating in the amplification of ATM-dependent DNA damage signals. *Mol. Cell.* 21:187–200.

Mari, P.O., B.I. Florea, S.P. Persengiev, N.S. Verkaik, H.T. Bruggenwirth, M. Modesti, G. Giglia-Mari, K. Bezstarosti, J.A. Demmers, T.M. Luider, et al. 2006. Dynamic assembly of end-joining complexes requires interaction between Ku70/80 and XRCC4. *Proc. Natl. Acad. Sci. USA.* 103:18597–18602.

Marples, B., B.G. Wouters, S.J. Collis, A.J. Chalmers, and M.C. Joiner. 2004. Low-dose hyper-radiosensitivity: a consequence of ineffective cell cycle arrest of radiation-damaged G2-phase cells. *Radiat. Res.* 161:247–255.

Redon, C., D. Pilch, E. Rogakou, O. Sedelnikova, K. Newrock, and W. Bonner. 2002. Histone H2A variants H2AX and H2AZ. *Curr. Opin. Genet. Dev.* 12:162–169.

Riballo, E., M. Kühne, N. Rief, A. Doherty, G.C. Smith, M.J. Recio, C. Reis, K. Dahm, A. Fricke, A. Krempler, et al. 2004. A pathway of double-strand break rejoining dependent upon ATM, Artemis, and proteins locating to gamma-H2AX foci. *Mol. Cell.* 16:715–724.

Rothkamm, K., and M. Löbrich. 2003. Evidence for a lack of DNA double-strand break repair in human cells exposed to very low X-ray doses. *Proc. Natl. Acad. Sci. USA.* 100:5057–5062.

Rothkamm, K., I. Krüger, L.H. Thompson, and M. Löbrich. 2003. Pathways of DNA double-strand break repair during the mammalian cell cycle. *Mol. Cell. Biol.* 23:5706–5715.

Rogakou, E.P., C. Boon, C. Redon, and W.M. Bonner. 1999. Megabase chromatin domains involved in DNA double-strand breaks in vivo. *J. Cell Biol.* 146:905–916.

Sengupta, S., A.I. Robles, S.P. Linke, N.I. Sinogeeva, R. Zhang, R. Pedeux, I.M. Ward, A. Celeste, A. Nussenzweig, J. Chen, et al. 2004. Functional interaction between BLM helicase and 53BP1 in a Chk1-mediated pathway during S-phase arrest. *J. Cell Biol.* 166:801–813.

Shiloh, Y. 2003. ATM and related protein kinases: safeguarding genome integrity. *Nat. Rev. Cancer.* 3:155–168.

Syljuasen, R.G., S. Jensen, J. Bartek, and J. Lukas. 2006. Adaptation to the ionizing radiation-induced G2 checkpoint occurs in human cells and depends on checkpoint kinase 1 and Polo-like kinase 1 kinases. *Cancer Res.* 66:10253–10257.

van Gent, D.C., J.H. Hoeijmakers, and R. Kanaar. 2001. Chromosomal stability and the DNA double-stranded break connection. *Nat. Rev. Genet.* 2:196–206.

Wahl, G.M., and A.M. Carr. 2001. The evolution of diverse biological responses to DNA damage: insights from yeast and p53. *Nat. Cell Biol.* 3:E277–E286.

Ward, I., and J. Chen. 2004. Early events in the DNA damage response. *Curr. Top. Dev. Biol.* 63:1–35.

Zhang, X., J. Succi, Z. Feng, S. Prithivirajsingh, M.D. Story, and R.J. Legerski. 2004. Artemis is a phosphorylation target of ATM and ATR and is involved in the G2/M DNA damage checkpoint response. *Mol. Cell. Biol.* 24:9207–9220.

Zhao, B., M.J. Bower, P.J. McDevitt, H. Zhao, S.T. Davis, K.O. Johanson, S.M. Green, N.O. Concha, and B.B. Zhou. 2002. Structural basis for Chk1 inhibition by UCN-01. *J. Biol. Chem.* 277:46609–46615.